

RECENT IMPROVEMENTS IN EXPERIMENTAL AND ANALYTICAL TECHNIQUES FOR THE DETERMINATION OF RELATIVE PERMEABILITY DATA FROM UNSTEADY STATE FLOW EXPERIMENTS

D.B.Bennion, Hycal Energy Research Laboratories Ltd.

F.B. Thomas, Hycal Energy Research Laboratories Ltd.

Copyright 1991, Society of Petroleum Engineers, Inc.

This paper was prepared for presentation at the SPE 10th Technical Conference and Exposition held in Port of Spain, Trinidad, June 26 - 28, 1991.

Summary. Accurate relative permeability data is an essential input parameter for many reservoir engineering applications, most significantly in the area of reservoir simulation. Methods of relative permeability determination are discussed with specific emphasis being given to the calculation of relative permeability curves from unsteady state displacement experiments. Recent advances in history matching techniques for the computation of relative permeability data from unsteady state displacement tests, including rigorous modeling of capillary effects, more flexible cubic and B spline functional forms for the relative permeability relations, and the simultaneous prediction of relative permeability and capillary pressure, are all discussed. Simple corrective techniques for correcting endpoint relative permeability values for in-situ capillary effects are also presented.

Introduction

Relative permeability is an empirical parameter used to modify Darcy's single phase flow equation to account for the numerous complex effects associated with the flow of multiple immiscible phases within porous media¹.

Relative permeability measurements are utilized extensively in many areas of reservoir engineering, and more particularly in recent years in the area of matching, predicting and optimizing reservoir performance and depletion strategies through the use of detailed numerical simulation models.

Those involved in numerical simulation realize the importance of good relative permeability data on the performance of reservoir simulation models. This paper discusses the evolution of relative permeability measurement techniques and reviews the current state of the art technology in the determination of relative permeability data. Recent experimental work and techniques for improving the acquisition of raw laboratory data for relative permeability calculations are also discussed.

Factors Affecting Relative Permeability

Relative permeability can be affected by many physical parameters including fluid saturations,²⁻⁴ physical rock properties,⁵⁻⁷ wettability,⁸⁻¹⁰ saturation history (hysteresis effects),^{11,12} overburden stress,^{13,14} clay and fines content,^{15,16} temperature,^{17,18} interfacial tension,¹⁹ viscosity,²⁰ magnitude of initial phase saturations,^{21,22} immobile or trapped phases,^{21,22} and displacement rates and capillary outlet phenomena.²³⁻²⁶ A detailed discussion of the many factors affecting relative permeability is beyond the scope of this paper, but the general consensus of researchers is that in order to obtain the most representative relative permeability data that reservoir conditions during the tests be duplicated as closely as possible. This involves the use of well preserved or restored state reservoir core material, the use of "live" uncontaminated actual reservoir fluids in the tests, and operation at full reservoir conditions of temperature, pressure and confining overburden stress.

Types of Relative Permeability Measurements

A number of researchers have postulated different methods for the experimental determination of relative permeabilities on reservoir core samples. The most popular of these fall into the category of "steady state" and "unsteady state" displacement tests. A number of centrifuge methods have also been proposed^{27,28} but in general have had limited acceptance due to the small size of the core samples which can be utilized and the inability to conduct those types of tests at reservoir conditions of temperature and pressure.

Steady State Measurements

Figure 1 provides an illustrative schematic of a typical steady state relative permeability apparatus. In this type of test a fixed ratio of two or more immiscible fluids are simultaneously forced through a test sample until saturation and pressure equilibrium are established. The experiments are designed in such a way as to eliminate end effects. This is accomplished in a number of ways, the most common being the inclusion of an additional length of core or sandpack to the end of the test section of interest to absorb the capillary end effect. Various other methods such as the use of semi-permeable membranes and plates, or cone shaped core ends to increase production velocity at the outlet face to minimize the end effect, have also been investigated.

At each equilibrium point, in a steady state test, individual-phase permeabilities and relative permeabilities are computed based on the measured phase differential pressures and individual phase flow rates. Once one set of stable data is obtained the injection ratio of the two fluids is varied, stability is re-established and the relative permeabilities at the next saturation level are then determined.

The steady-state method is preferred by some investigators since end effects are negated and, since the test is not truly a displacement test but rather an equilibrium flow test, stability and rate effects associated with viscous instabilities are eliminated. The disadvantages of this method are:

1. Accurate determination of in-situ saturations is required after each displacement level which can be difficult and expensive in reservoir condition tests.

2. Days or weeks are often required to achieve equilibrium at each saturation point. This can result in weeks or months being required to complete a simple relative permeability determination at an extremely high cost.
3. A considerable amount of expensive experimental equipment is required to conduct these tests, particularly at conditions of elevated temperature and pressure.

Unsteady State Measurements

These much simpler tests are conducted rapidly by the displacement of a single phase through a core which is initially saturated with wetting and non-wetting phase and is at the minimum saturation of the phase to be injected (ie. S_{wi} for a waterflood in a water-wet core). The production history and pressure differential across the core are closely monitored during the displacement. Mathematical derivations of classical Buckley-Leverett²⁹ theory or more complex computer simulation techniques, (which shall be discussed shortly), can be used with this data to compute the relative permeability curves. Because this type of experiment can be conducted relatively rapidly and at a low cost, it is almost exclusively utilized in preference to the steady-state method for commercial relative permeability testing. The main disadvantages of this method are its susceptibility to end effects, rate-dependent instability effects, and potential non-equilibrium between displacing and displaced fluids.

Calculation Methods for Computation of Relative Permeability From Laboratory Data

Steady-State Methods

As discussed previously, relative permeabilities can be computed directly from two-phase steady-state relative permeability displacement tests at given saturation levels. This is a distinct advantage of the steady-state method as no special treatment or manipulation of the data is required. Due to the cost and complexity of steady state measurements; however, they are not often utilized with preference being given to the much simpler and less expensive unsteady state test.

Unsteady-State Methods

The fluid theory initially described by Buckley and Leverett²⁹ to describe fluid flow through porous media was later modified by Welge³⁰ to facilitate the prediction of relative permeability ratios at given saturation levels in laboratory scale core displacement tests. These classical flow equations are described in detail in the above references, to which the reader is referred.

For the case of horizontal flow and negligible capillary pressure, Welge illustrated that:

$$S_{w,av} - S_{w,2} = F_{o_2} Q_w \quad (1)$$

where:

$S_{w,av}$ = average core water saturation
 $S_{w,2}$ = outlet-face water saturation
 F_{O_2} = fractional flow of oil at outlet face
 Q_w = total pore volumes of water injected

Since $S_{w,av}$ and Q_w are known (from material balance and injection data respectively) and F_{O_2} can be determined from a plot of Q_w as a function of $S_{w,av}$ it can be calculated that:

$$f_{o_2} = \frac{1}{1 + \frac{\mu_o/k_{ro}}{\mu_w/k_{rw}}} \quad (2)$$

where:

μ_o, μ_w = oil and water viscosities (cP)
 k_{ro}, k_{rw} = endpoint oil and water relative permeability values.

This allows the relative permeability ratio to be computed at any saturation AFTER breakthrough of the water phase. Similar equations can be derived for gas-oil systems.

The work of Welge was extended by Johnson *et al*³¹ to obtain a method (commonly called the JBN method) for calculating individual-phase relative

permeabilities from unsteady-state test data. These equations are:

$$k_{ro} = \frac{f_{o_2}}{d\left(\frac{1}{Q_w I_r}\right)/d\left(\frac{I}{Q_w}\right)} \quad (3)$$

$$k_{rw} = \frac{f_{w2}}{f_{O_2}} \frac{\mu_w}{\mu_o} k_{ro} \quad (4)$$

$$I_r = \frac{\text{injectivity}}{\text{initial injectivity}} = \frac{Q_{wi}/\Delta P}{(Q_{wi}/\Delta P)_{init}} \quad (5)$$

where:

F_{w2} = outlet fractional flow of water
 ΔP = pressure differential across sample

The advantage of the JBN method over that of the Welge method was that for the first time individual phase relative permeabilities could be computed from unsteady state data instead of merely relative permeability ratios.

The JBN method has been popular since its inception, even though it suffers from some basic deficiencies, and is still used in many applications today.

Another fairly popular method is that of Jones and Roszelle³². This method is an extension of the JBN method and also utilizes graphical techniques (which can be computerized).

The basic assumptions of the Jones-Roszelle method are similar to that of the previously discussed JBN method. In this technique the oil produced is expressed as a change in the average water saturation within a core sample. The change in saturation is plotted vs the pore volumes of water injected to calculate the relative permeability ratios as a function of the water saturation.

The Jones-Roszelle method has particular application late in waterfloods when oil production is very minimal and the slope of the oil recovery vs PV of injection graph becomes very slight. The methods involve plotting recovery vs the inverse of cumulative injection ($1/Q_{wi}$) which avoids long tangent extrapolations back to the y axis and also facilitates easy extrapolation back to the point of infinite water injection ($1/Q_{wi} = 0$), which is thought by the authors to yield a better estimation of the true residual oil saturation after a waterflood.

Since all three methods discussed previously are based upon the same fundamental derivations of Buckley-Leveritt flow theory, they tend to be subject to the same limitations, namely:

1. All methods neglect both capillary pressure and gravitational effects in their basic derivation. This means that the methods cannot account for end effect phenomena and the dispersing effect of capillary pressure on saturation shock fronts within porous media. Typically in the past these types of tests were run at very high displacement velocities to yield a large pressure drop across the core sample to minimize the contribution of capillary pressure effects. This can lead to severe problems with both fines mobilization and viscous instability effects.
2. The Welge, JBN and Jones-Roszelle methods all assume perfectly dispersed flow with no core heterogeneities. Since these methods are based on the evaluation of derivatives of the fractional flow curves, if the fractional flow data is non-monotonic, which can often occur in heterogeneous core samples, this results in severe deviations in the computed relative permeability data. This phenomena is illustrated by Sigmund *et al*³³ and appears as Figure 3.
3. Since all of the methods are based upon the analysis of fractional flow data, they can only predict relative permeability data after water breakthrough. In strongly water wet core material, a water displacement results in an almost piston like flow of water through the core resulting in a very steep and localized region of fractional flow. This, therefore, results in only a very small cluster of relative

permeability data points being obtained at saturations near the maximum level. Thus significant extrapolation is required for the relative permeabilities at intermediate saturation levels.

This last deficiency was commonly remediated by utilizing a viscous mineral oil in place of the hydrocarbon phase in the test. This, however, yields an improper viscosity ratio which can affect residual saturations and endpoint relative permeability values. Also, the use of refined or synthetic oils can affect core wettability due to the solubilization of asphaltic and heavy ends into solution and cause significant changes in the configuration of the resulting relative permeability curves.

The drawback of the previous three calculation methods is that, since classical behavior is assumed in the method derivations (i.e. no capillary pressure, no end effects, perfectly dispersed flow with no heterogeneities), the accuracy of the obtained relative permeabilities can, in many instances, be questionable.

The implicit history matching technique, first proposed by Archer and Wong³⁴ is an offshoot of the large advances recently made in reservoir simulation. The basis of the method is that, instead of using known relative permeability relationships in the solution of the partial differential equations which describe multi-phase flow in porous media to predict the pressure and production history, the pressure and production history is utilized to predict the relative permeability curves for a given system.

The method begins by assuming certain functional relationships in the simulator for the wetting and non-wetting phase relative permeabilities and the capillary pressure functions. Initial estimates for adjustable parameters in these equations result in a certain production and pressure history being predicted. This production and pressure history is then compared to the input experimental lab data and the least-square error computed. Correction algorithms adjust the parameters in the functional relationships and the process continues to iterate in this fashion until the minimum least-square error is obtained. The resulting relative permeability curves obtained provide the best fit (within the limits set by the form of the functional relationships utilized) to the experimental data.

Since the numerical model can incorporate both gravity and capillary pressure effects, these can be incorporated directly into the simulation thus allowing the end effect to actually be simulated as a portion of the experiment. This facilitates running tests at low advance rates to eliminate stability problems. The method also provides a complete history match over the entire range of the saturation change, regardless of the fractional flow characteristics of the displacement, giving it specific application to heterogeneous and strongly wetted systems.

The first published applications of the method were presented by Sigmund and McCaffery.³³ They utilized relatively simple exponential formulations to define the functional form for the relative permeability curves as follows:

$$k_{rw} = k_{rwo} \left[\frac{(Se)^{\epsilon_w} + ASe}{1 + A} \right] \quad (6)$$

$$k_{mw} = k_{mwo} \left[\frac{(1-Se)^{\epsilon_n} + B(1-Se)}{1 + B} \right] \quad (7)$$

$$Se = \frac{Sw - Sw_{\min}}{Sw_{\max} - Sw_{\min}} \quad (8)$$

where:

- k_{rw} = Predicted wetting phase relative permeability
- k_{rwn} = Predicted non-wetting phase relative permeability
- k_{rwo} = Wetting phase endpoint relative permeability
- k_{mwo} = Non-wetting phase endpoint relative permeability
- ϵ_w = Wetting phase adjustable shape exponent
- ϵ_n = Non-wetting phase adjustable shape exponent
- A, B = Linearization constants (0.01 in Sigmund's work)

- Se = Normalized wetting phase saturation
- Sw = Wetting phase saturation
- Sw_{\min} = Minimum wetting phase saturation
- Sw_{\max} = Maximum wetting phase saturation

Capillary pressure effects were expressed by:

$$P_c = P_{cb} \left[\frac{1}{(S_{pc})^{1/\lambda}} - 1 \right] \quad (9)$$

where:

$$S_{pc} = \frac{S_w - S_{wi}}{S_{wo} - S_{wi}} \quad (10)$$

- P_c = Capillary pressure
- P_{cb} = Measure of interfacial tension and mean pore size
- λ = Pore size distribution parameter
- S_{pc} = Normalized capillary pressure saturation value
- Sw_i = Irreducible wetting phase saturation from a drainage capillary pressure test. (Always must be less the Sw_{\min}).
- Sw_o = Maximum value of wetting phase saturation corresponding to zero capillary pressure.

The numerical model utilized to match the data incorporated the one-dimensional Buckley-Leverett, incompressible, two phase flow equations;

$$\frac{k}{\mu_w} \frac{\partial}{\partial x} \left(k_{rw} \frac{\partial P_w}{\partial x} \right) = \phi \frac{\partial Sw}{\partial t} + q_{iw} \quad (11)$$

$$\frac{k}{\mu_{mw}} \frac{\partial}{\partial x} \left(k_{mw} \frac{\partial P_{mw}}{\partial x} \right) = -\phi \frac{\partial Sw}{\partial t} + q_{mw} \quad (12)$$

$$P_c = P_{nw} - P_w \quad (13)$$

where:

k	=	Absolute permeability
μ_w, μ_n	=	Viscosities of wetting and non-wetting phases
k_{rw}	=	Relative permeability of wetting phase
k_{rnw}	=	Relative permeability of non-wetting phase
P_w	=	Pressures in the wetting phase
P_{nw}	=	Pressures in the non-wetting phase
ϕ	=	Porosity
S_w	=	Wetting phase fraction
q_{iw}	=	Source terms for wetting phase
q_{inw}	=	Source terms for non-wetting phase
P_c	=	Capillary pressure
∂_x	=	Space co-ordinate
∂_t	=	Time co-ordinate

The model utilized by Sigumund et al utilized one-point upstream transmissibility weighting with linearized implicit transmissibilities (utilizing a secant method to estimate the derivatives) and a modified Newtons method to handle capillary pressure induced non linearities. A 40 gridblock one dimensional model was utilized.

The optimum relative permeability parameters were calculated using a least squares Gauss-Newton optimization routine. The error equation for the i_{th} observation in this routine can be written as:

$$Error = \Delta P_{OBC_i}^q + \Delta E_{OBC_i}^q \quad (14)$$

where:

$$\Delta P_{OBC_i}^q(\epsilon_w, \epsilon_{nw}) = W_i \left(\Delta P_{D_i}^{obs} - \Delta P_{D_i}^{Calc} \right) \quad (15)$$

and

$$\Delta E_{OBC_i}^q(\epsilon_w, \epsilon_{nw}) = W_i \left(E_{R_i}^{obs} - E_{R_i}^{calc} \right) \quad (16)$$

where:

W_i	=	Weighting factor
P_D	=	Pressure data
E_R	=	Recovery data
obs	=	Measured data
$calc$	=	Calculated data
obc	=	Objective function

For a given set of "m" observations (data points) the algorithm attempts to find the values of ϵ_w and ϵ_{nw} which will minimize the error function:

$$E = \sum_{i=1}^m \left[\left(\Delta P_{OBC_i}^q \right)^2 + \left(\Delta E_{OBC_i}^q \right)^2 \right] \quad (17)$$

subject to the given constraints;

$$\epsilon_{min} \leq \epsilon_w, \epsilon_{nw} \leq \epsilon_{max}$$

Details of the specific application of the Gauss-Newton correction algorithm can be found in the appendix of Sigumund et al.³³

Batycky *et al*²⁴ and MacMillan³⁵ also utilized this technique using similar functional forms.

One disadvantage of this particular form of the history matching method is that the obtained relative permeability curves can conform to only the configurations possible under the constraints imposed by the given functional form. The exponential forms discussed previously are usually quite adequate for most systems, but cannot adequately model unusual relative permeability configurations, such as those obtained for dual porosity or very heterogeneous systems. Figure 4 provides an illustration of the various types of relative permeability curve configurations which can be obtained using different values of ϵ_w and ϵ_{nw} in the exponential formulation model.

The history matching technique, however, is

not limited to the use of any one specific functional relationship. Research by Kerig *et al*^{36,37} indicated that free and clamped cubic spline formulations could provide superior fits to almost all types of relative permeability curves.

Kerig *et al* utilized a cubic spline functional form to represent the relative permeability curves defined by:

$$k_{ri} = a_{ij}S_i^3 + b_{ij}S_i^2 + c_{ij}S_i + d_{ij} \quad (18)$$

For $S_{i,j} \leq S_i \leq S_{i,j+1}$

Where:

- J = number of total spline segments
- $S_{i,j}$ = Value of S_i at knot J
- a_{ij} = spline coefficient
- b_{ij} = spline coefficient
- c_{ij} = spline coefficient
- d_{ij} = spline coefficient

Cubic splines are highly flexible functions which can, with a sufficient number of spline segments, represent any continuous function as accurately as desired³⁸. Figure 5 illustrates the flexibility of cubic splines in modeling relative permeability curves of a nonuniform nature which cannot be well described by simple exponential formulations. Examples of such system would include very heterogeneous reservoirs or systems characterized by multiple porosity types.

Kerig *et al*³⁷ discussed sources of error in the relative permeability estimation technique via automatic history matching. They defined two possible sources of error:

1. Modeling Error - Results of inadequacy of the mathematical model of the displacement experiment in the exact representation of the experiment (ie. effect of capillary pressure, heterogeneity or non-uniform initial saturation).
2. Estimation Error
 - a) Bias Error - Inability of the functional forms to represent the true, though unknown, relative permeability curves.

- b) Variance Error - errors associated with statistical uncertainty of the data utilized (i.e. experimental error) and the number of parameters utilized in the functional form of the relative permeability curves. (Increasing the number of parameters in the functional form generally increases the variance error while reducing the bias error.)

The use of cubic spline formulations over simple exponential formulations can greatly reduce bias error while causing relatively small increases in variance error as illustrated in Figure 6.

Kerig *et al*³⁹ did additional work in this area and determined specific algorithms for the optimization of the many parameters required when cubic splines are utilized as functional forms in the relative permeability relations. The algorithms utilized incorporated inequality constraints to ensure that physically realistic relative permeability curves were maintained throughout the optimization process. The constraints utilized were such to ensure that the relative permeability curves obtained remained convex downward, remained monotonic, and had zero relative permeability at $S_i = 0$. The optimization program utilized in this work was a Gauss-Newton method with a Marquart modification^{40,41}. A detailed discussion of the model and operational constraints utilized can be found in Reference 39.

Watson *et al*⁴² further extended this work to include the use of B Splines³⁸ as functional forms for the relative permeability curves using:

$$k_{ri}(S_i) = \sum_{j=1}^{N_i} C_j^i B_j^m(S_i) \quad i = w, nw \quad (19)$$

- N_i = Dimensions of the Spline
- C_j^i = Parameters to be determined

The use of B Splines has an advantage over the use of Cubic Splines in that B Splines are not "piecewise" type polynomial approximations (ie. each spline segment is valid only over a certain saturation interval). B Splines retain a set of independent coefficients over the entire saturation range of interest making them easier to use while still retaining the

flexible nature of cubic splines. The algorithms utilized and operational constraints employed during the optimization process are discussed in detail by Watson *et al.*⁴² Figure 7 illustrates the superior nature of spline estimated relative permeability data over that predicted by simple exponential models.

Richmond *et al.*⁴³ further extended the work of Watson *et al.*⁴² to include simultaneous optimization of capillary pressure data along with the prediction of relative permeabilities from displacement experiments. The functional form for the capillary pressure was also defined by B Splines as:

$$P_{c_i}(S_i) = \sum_{j=1}^{N_i} C_j^i B_j^m(S_i) \quad (20)$$

Richmond *et al.*⁴³ utilized a Levenberg-Marquart Algorithm with linear inequality constraints in their optimization process. They also investigated the problem of convergence on multiple distinct local minima by variation of their initial optimization initialization point and covariance analysis of the Hessian matrix obtained from the solution of the data. Also proposed was a new procedure for the automatic selection of the optimum number and location of the spline knots to obtain the maximum accuracy in estimation with the minimum number of spline segments and resulting optimizations.

The work of Richmond *et al.* utilized pure parameter adjustment for the history matching of the capillary pressure functions to optimize the error between the experimentally observed pressure and production history and the simulator predicted data. Recent research at Hycal has been involved in the actual measurement of in-situ capillary pressures during a dynamic displacement test through the use of pressure transducers equipped with special wetted membranes to sense specific individual phase pressures and the resulting capillary pressure.

The measurement of actual dynamic capillary pressure data allows the further extension of the history matching technique to the direct history matching of the capillary pressure curve allowing for the direct prediction of both reservoir condition relative permeabilities and capillary pressures accurately and inexpensively from a single test.

Further testing and experimentation is still under way to continue to improve and refine this latest addition to the history matching method.

Simple Correction Techniques for Endpoint Relative Permeability Values

All of the history matching models previously discussed require that the user input both the wetting and non wetting phase endpoint relative permeability values. Relative permeability endpoint values, determined utilizing a standard unsteady state displacement technique, may often result in the measurement of endpoint values which are substantially lower than actual values measured from steady state tests. Figure 8⁴⁴ illustrates this phenomena for displacement tests conducted at the same rate utilizing both a Penn-State type steady state approach vs the standard unsteady-state test methodology.

The major cause of this type of phenomena is attributed to capillary effects. An excellent discussion of capillary and rate effects can be found in the work of Batycky²⁴, Osaba⁴⁵, and Rapoport and Leas.⁴⁶

Capillary pressure is simply defined as:

$$P_c = P_{nw} - P_w \quad (21)$$

where:

$$\begin{aligned} P_c &= \text{Capillary pressure (kPa/psi)} \\ P_{nw} &= \text{Non-wetting phase pressure (kPa/psi)} \\ P_w &= \text{Wetting phase pressure (kPa/psi)} \end{aligned}$$

When a single fluid is flowing in the porous media in the presence of other immobile residual immiscible fluid phases (i.e. the flow of water at a residual oil saturation), a certain portion of the applied force to move the fluid through the system is required to overcome the capillary forces which exist within the sample. Generally, the larger the capillary forces which exist within a sample, the larger the influence on the endpoint relative permeability data.

Typically in the past relative permeability tests were conducted at high rates which resulted in a relatively large pressure differential across the core sample which, in general was much larger than the

capillary pressure force and thus tended to minimize its overall effect on the measured endpoint relative permeability value. Figure 9⁴⁴ provides an illustrative example of this phenomena.

The use of high rates in conducting unsteady state relative permeability tests has associated problems, these being:

1. The potential for fines migration.
2. Unstable flow effects due to viscous instability.²³
3. Erroneous pressure data due to non-Darcy flow caused by turbulent interstitial flow.
4. Experimental data acquisition difficulties resulting from a very short test time.

Recent work has illustrated that a simple correction technique can be accurately applied to correct for the effect of capillary effects on endpoint relative permeabilities while avoiding many of the aforementioned difficulties. The technique is applied as follows:

1. Conduct a regular, low rate unsteady state displacement test, measure the resulting endpoint relative permeability and residual fluid saturations.
2. Use the computer history matching routine to generate the complete relative permeability curves.
3. Conduct geometric rate increases of the displacing phase at 2 to 3 higher displacement velocities. Example, if the base displacement test was conducted at a rate of 10 mL/hr, conduct additional endpoint tests at 20, 40 and 80 mL/hr. The technique does not require the use of excessively high injection rates and these should be avoided to reduce the potential for fines mobilization or unstable flow.
4. Record any additional production of the residual immobile phase caused by the increase in interstitial fluid shear force.

The profile of the experimental results can have three configurations as illustrated in Figure 10, these being:

CASE 1 - Endpoint permeability remains constant with rate illustrating perfect conformance to Darcies Law indicating an absence of capillary effects. This indicates that no correction of the endpoint relative permeability data is required and that capillary effects are negligible.

CASE 2 - Endpoint permeability increases with increasing injection rate. This indicates the presence of capillary forces, a reduction in the residual immobile phase saturation, or a combination of both phenomena. The endpoint correction technique, to be discussed shortly, should be applied here.

CASE 3 - Endpoint permeability decreases or initially increases then decreases with increasing injection rate. This indicates either damage by fines mobilization or turbulent flow phenomena. These two phenomena can be easily differentiated by reducing to the base rate and observing if the permeability returns to the originally recorded value. In the case of fines migration the endpoint correction technique, in general, can still be applied if sufficient points (3 minimum) are available prior to the reduction in permeability. If turbulent flow occurs, lower rates should be selected to allow evaluation in the laminar flow regime.

The correction technique is applied by fitting the non linear model:

$$k_i = a_1(1 - e^{-a_2 q_i}) \tag{22}$$

where:

- k_i = measured endpoint permeability at flow rate "i" (mD or μm^2)
- q_i = flow rate at point "i" (cc/hr, cc/sec)
- a_1, a_2 = adjustable constants

to the experimentally determined data. In this work a non-linear finite difference Levenberg-Marquardt optimization routine^{41,47-49} was used to optimize the values of the constants a_1 and a_2 to yield the minimum least square error between the experimental and predicted data.

By definition, as the flowrate, q_i approaches infinity, the pressure across the sample also becomes infinitely larger than any contribution associated with capillary effects. Thus,

$$\lim_{q_i \rightarrow \infty} a_1(1 - e^{-a_2 q_i}) = a_1 \quad (23)$$

Thus the value of the constant a_1 provides the simple final approximation to the final corrected permeability value. Examples of the application of this technique for both water oil and gas-oil displacement tests appear as Tables 1 and 2 and Figures 11 and 12. The resulting relative permeability data is simply renormalized at this point to the higher endpoint relative permeability value.

If the residual immobile phase saturation is reduced by the elevated rate displacements, as may sometimes occur due to the increase in capillary number associated with the higher displacement velocity. This is accommodated by (See Figure 13):

1. Determine "new" final residual saturation.
2. Using the previously derived and matched functional form for the relative permeability curve, extrapolate the existing relative permeability curve to the "new" residual saturation.
3. Normalize the new set of relative permeability data up to the final corrected endpoint relative permeability.

Use of this technique eliminates the use of high displacement rates during the actual two phase immiscible displacement test which obviates the potential for viscous instability effects. Since the method works upon an extrapolative technique, this also eliminates the need for extreme flow velocities to facilitate the endpoint correction, and thus has specific application to velocity sensitive core materials.

Conclusions

Recent advances in unsteady state displacement technology have allowed the data from these relatively simple and inexpensive tests to have much wider application and improved accuracy when correlated with the data from more expensive and time consuming steady state tests. Advances have

been made in automatic history matching, particularly with the advent of more sophisticated cubic spline and B spline functional forms for the relative permeability and capillary pressure relations. Recent work also indicates the possibility of the prediction of accurate reservoir condition capillary pressures simultaneously during unsteady state displacement tests. Simple procedures for the correction of endpoint relative permeability data by the use of parameter estimation techniques to match the results of multirate flow tests were documented and illustrative examples of the technique presented.

References

1. Muskat, M., and Meres.: M.W.: *Physics*, Vol. 7, (1936) 346.
2. Leverett, M.C., and Lewis, W.B.: "Steady Flow of Gas-Oil-Water Mixtures Through Unconsolidated Sands," *Trans.*, AIME, Vol. 142 (1941) 107.
3. Sarem, A.M.: "Three Phase Relative Permeability Measurements by Unsteady State Methods," *SPEJ*, Vol. 9 (1966) 199.
4. Owens, W.W. and Archer, D.E.: "The Effect of Rock Wettability on Oil-Water Relative Permeability Relationships," *Trans.*, AIME (July 1971) 873-78.
5. Maloney, D.R., Honarpour, M.M., Brinkmeyer, A.D.: "The Effects of Rock Characteristics on Relative Permeability," NIPER Report No. FC22-83 FE 60149 (January 1990).
6. Morrow, N.R.: "Capillary Pressure Correlation for Uniformly Wetted Porous Media," *JCPT*, (Oct. 1976).
7. Arps, J.J. and Roberts, T.G.: "The Effect of the Relative Permeability Ratio, the Oil Gravity and the Solution Gas-Oil Ratio on the Primary Recovery from a Depletion Type Reservoir," *Trans.*, AIME Vol. 24 (1955) 120.

8. Craig, F.F., Jr.: "The Reservoir Engineering Aspect of Waterflooding," *SPE Monogram Series* (1971).
9. Wang, F.H.L.: "Effect of Wettability Alteration on Water/Oil Relative Permeability, Dispersion, and Flowable Saturation in Porous Media," *SPE Res. Eng.* (May 1988).
10. Morrow, N.R., Lim, H.T., Ward, J.S.: "Effect of Crude Oil Induced Wettability Changes on Oil Recovery," *SPE Form. Eval.* (Feb. 1986).
11. Geffen, T.M., Owens, W.W., Parrish, D.R., and Morse, R.A.: "Experimental Investigation of Factors Affecting Laboratory Relative Permeability Measurements," *Trans., AIME*, Vol. 192, (1951) 99.
12. Land, C.S.: "Comparison of Calculated and Experimental Imbibition Relative Permeability," *Trans., AIME*, Vol. 251 (1971) 419.
13. Wei, K.K., Morrow, N.R., Brower, K.R.: "Effect of Fluid, Confining Pressure and Temperature on Absolute Permeabilities of Low Permeability Sandstones," *SPE Form Eval.* (August 1986).
14. Gobran, B.D., Brigham, W.E., Ramey, J.H. Jr.: "Absolute Permeability as a Function of Confining Pressure, Pore Pressure, and Temperature," *SPE Form. Eval.*, (March 1987).
15. Soeder, D.J.: "Laboratory Drying Procedures and The Permeability of Tight Sandstone Core," *SPE Form. Eval.* (February 1986).
16. Selby, R.J., Ali, S.M.F.: "Mechanics of Sand Production and the Flow of Fines in Porous Media," *JCPT*, (May 1988).
17. Nakornthorp, K., Evans, R.D.: "Temperature Dependant Relative Permeability and Its Effect on Oil Displacement by Thermal Methods," *SPE Res. Eng.*, (May 1986) 230-242.
18. Polikar, M., Ali, S.M.F., Puttagunta, V.R.: "High Temperature Relative Permeabilities For Athabasca Oil Sands," *SPE Res. Eng.* (Feb. 1990).
19. Morrow, N.R., Chatzes, I., Taber, J.J.: "Entrapment and Mobilization of Residual Oil in Bead Packs," *SPE Res. Eng.* (1988).
20. LeFebvre duPrey, E.J.: "Factors Affecting Liquid-Liquid Relative Permeabilities of Consolidated Porous Medium," *SPEJ* 2, (1973) 39.
21. Caudle, B.H., Slobod, R.L., and Brownscombe, E.R.: "Further Developments in the Laboratory Determination of Relative Permeability," *Trans., AIME*, Vol. 192 (1951) 145.
22. McCaffery, F.G.: "The Effect of Wettability on Relative Permeability and Imbibition in Porous Media," Ph.D. Thesis, University of Calgary, Alberta, Canada (1973).
23. Sigmund, P., Sharma, H., Sheldon, D. and Aziz, K.: "Rate Dependence of Unstable Waterfloods," *SPE Res. Eng.* (May 1988).
24. Batycky, J.P., McCaffery, F.G., Hodgous, P.K. and Fisher, D.B.: "Interpreting Relative Permeability and Wettability from Unsteady State Displacement Measurements," *SPEJ*, (June 1981) 296.
25. Peters, E.J., and Flock, D.L.: "The Onset of Instability During Two-Phase Immiscible Displacement in Porous Media," *SPEJ*, (April 1981) 249.
26. Bentsen, R.G.: "A New Approach to Instability Theory in Porous Media," *SPEJ*, (Oct. 1985) 765.
27. Van Spronsen, E.: "Three-Phase Relative Permeability Measurements Using the Centrifuge Method." Paper SPE/DOE 10688 Presented at the Third Joint Symposium, Tulsa, Okla. (1982).

28. O'Mera, D.J., Jr. and Lease, W.O.: "Multiphase Relative Permeability Measurements Using an Automated Centrifuge," Paper SPE 12128 Presented at the SPE 58th Annual Technical Conference and Exhibition, San Francisco (1983).
29. Buckley, S.E. and Leverett, M.D.: "Mechanism of Fluid Displacement in Sands," *Trans.*, AIME, Vol. 146 (1942) 107.
30. Welge, H.J.: "A Simplified Method for Computing Recovery by Gas or Water Drive," *Trans.*, AIME, Vol. 195 (1952) 91.
31. Johnson, E.F., Bossler, D.P., and Nauman, V.O.: "Calculation of Relative Permeability from Displacement Experiments," *Trans.*, AIME, Vol. 216, 2959, 370.
32. Jones, S.C. and Rozelle, W.O.: "Graphical Techniques for Determining Relative Permeability from Displacement Experiments," *JPT*, Vol. 15 (1978) 807.
33. Sigmund, P.M., and McCaffery, F.G.: "An Improved Unsteady-State Procedure for Determining the Relative Permeability Characteristics of Heterogeneous Porous Media," *SPEJ* (Dec. 1973) 343.
34. Archer, J.S., and Wong, S.W.: "Use of a Reservoir Simulator to Interpret Laboratory Waterflood Data," *SPEJ*, (Dec. 1973) 343.
35. M^{ac}Millan, D.J.: "Automatic History Matching of Laboratory Corefloods to Obtain Relative Permeability Curves," *SPEJ*, (February 1987) 85.
36. Kerig, P.D.: "Estimation of Relative Permeabilities from Displacement Experiments," Ph.D. Dissertation, Texas A & M Univ., College Station, Texas (1985).
37. Kerig, P.D., Watson, A.T.: "Relative Permeability Estimation from Displacement Experiments: An Error Analysis," *SPE Res. Eng.* (March 1986).
38. Schumaker, L.L.: *Spline Functions: Basic Theory*, John Wiley and Sons Inc., New York (1981).
39. Kerig, P.D. and Watson, A.T.: "A New Algorithm for Estimating Relative Permeabilities From Displacement Experiments," *SPE Res. Eng.*, (1987).
40. Bard, Y.: *Nonlinear Parameter Estimation*, Academic Press, New York (1974).
41. Marquart, D.W.: "An Algorithm for Least Squares Estimation of Non-Linear Parameters," *Soc. Industrial Applied Math Journal*, (1963).
42. Watson, A.T., Richmond, P.C., Kerig, P.D. and Tao, T.M.: "A Regression Based Method for Estimating Relative Permeabilities from Displacement Experiments," *SPE Res. Eng.* (1988).
43. Richmond, P.C. and Watson, A.T., "Estimation of Multiphase Flow Functions From Displacement Experiments," *SPE Res. Eng.* (1990).
44. Fassihi, M.R., "Estimation of Relative Permeability from Low Rate Unsteady State Tests - A Simulation Approach," *JCPPT*, (May 1989).
45. Osaba, J.S.: "Laboratory Measurements of Relative Permeability," *Trans.*, AIME Vol. 192 (1951) 47.
46. Rapoport, L.A., and Leas, W.J.: "Relative Permeability to Liquid in Liquid-Gas Systems," *Trans.*, Vol. 192 (1951).
47. Brown, K.M., and Dennis, J.E.: "Derivative Free Analogues of the Levenberg- Marquardt and Gauss Algorithms for Nonlinear Least Squares Approximations," *Numerische Mathematik*, 18 (1972) 289-297.

48. Brown, K.M.: "Computer Oriented Methods for Fitting Tabular Data in the Linear and Nonlinear Least Squares Sense," Department of Computer, Information, and Control Sciences, TR No. 72-13, University of Minnesota.
49. Levenberg, K.: "A Method for the Solution of Certain Non-Linear Problems in Least Squares," *Quart. Appl. Math.* 1, (1944) 164-168.

TABLE 1
CORE AND FLUID PARAMETERS
FOR ENDPOINT CORRECTION TESTS

	Core "A"	Core "B"
Length (cm)	5.45	4.85
Diameter (cm)	3.80	3.80
Porosity (%)	21.0	17.2
Water Viscosity (cP)	0.581	0.581
Live Oil Viscosity (cP)	3.78	3.78
Gas Viscosity (cP)	0.0124	0.0124

TABLE 2
ENDPOINT CORRECTION TEST DATA

CORE "A"			
Injection Rate (mL/hr)	Endpoint Permeability To Water (mD)	Injection Rate (mL/hr)	Endpoint Permeability To Gas (mD)
10	1.85	20	0.825
20	2.37	50	2.79
50	4.07	100	3.56
100	6.82	200	4.69
200	10.98	500	7.69
Extrapolated Endpoint Permeability	14.50		7.92
CORE "B"			
Injection Rate (mL/hr)	Endpoint Permeability To Water (mD)	Injection Rate (mL/hr)	Endpoint Permeability To Gas (mD)
5	2.55	10	3.61
20	4.43	20	7.10
40	6.62	50	9.35
80	9.59	100	9.90
200	13.17		
Extrapolated Endpoint Permeability	13.27		10.03

FIGURE 1
STEADY-STATE RELATIVE PERMEABILITY APPARATUS

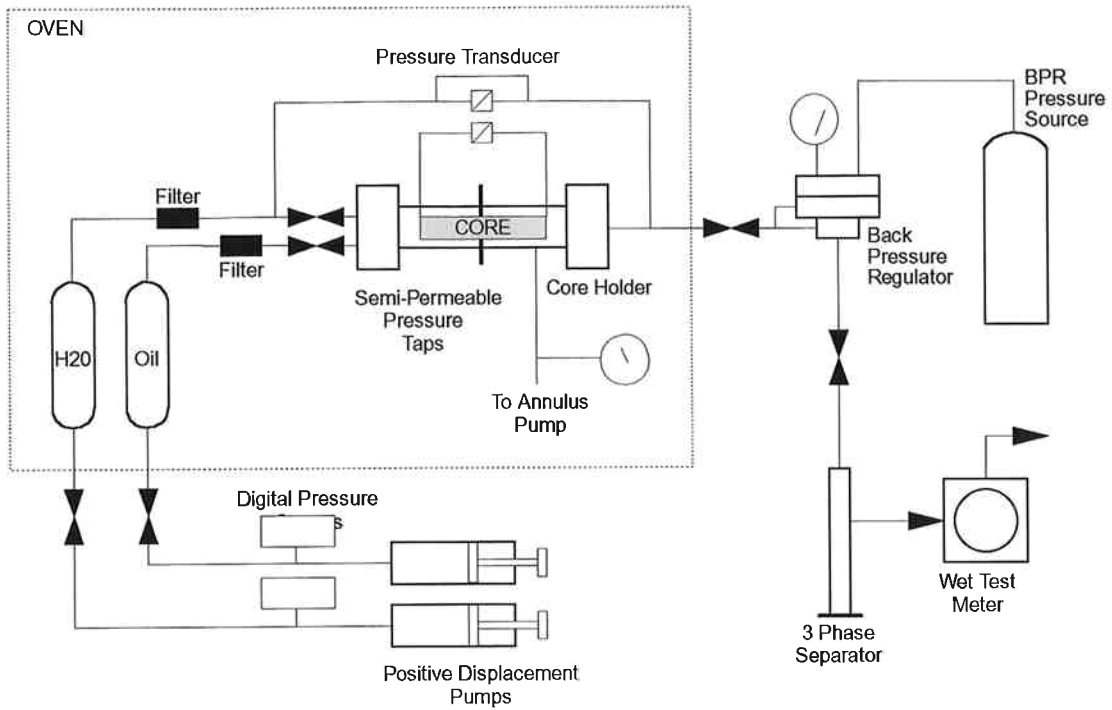


FIGURE 2
UNSTEADY-STATE RELATIVE PERMEABILITY APPARATUS

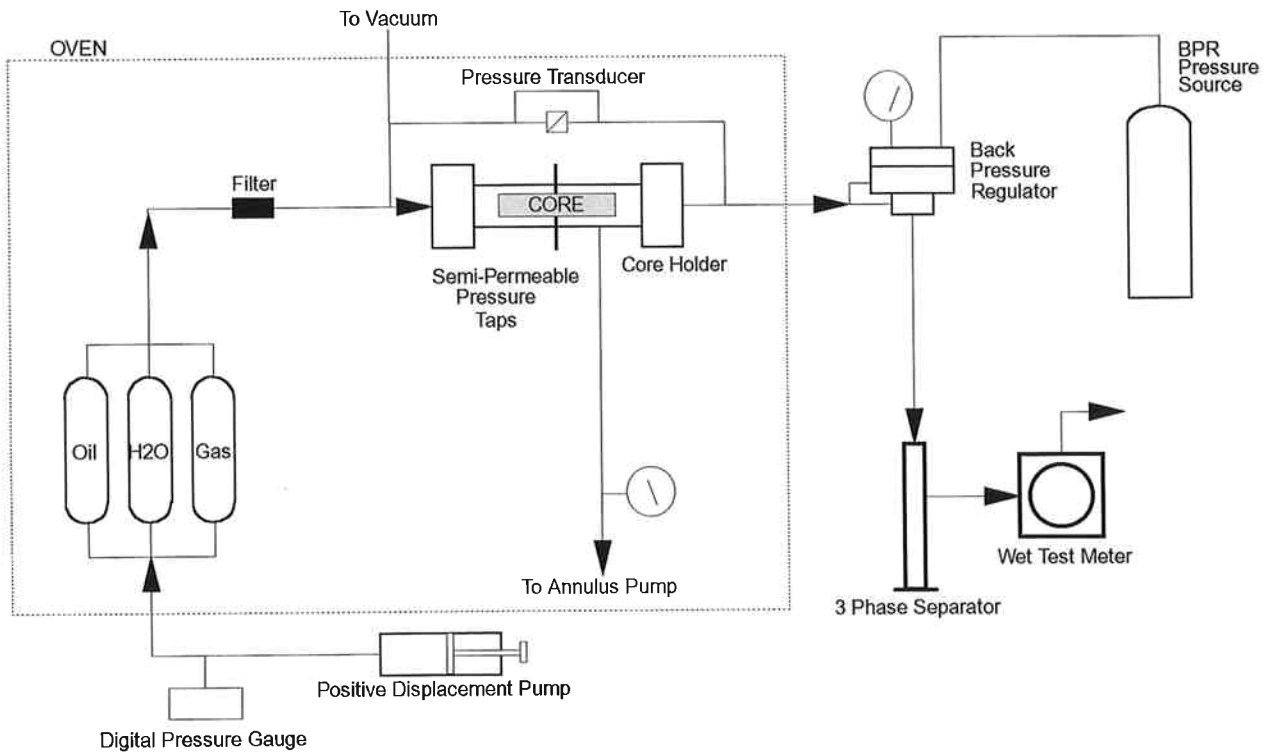


FIGURE 3
IMBIBITION RELATIVE PERMEABILITY
JBN METHOD

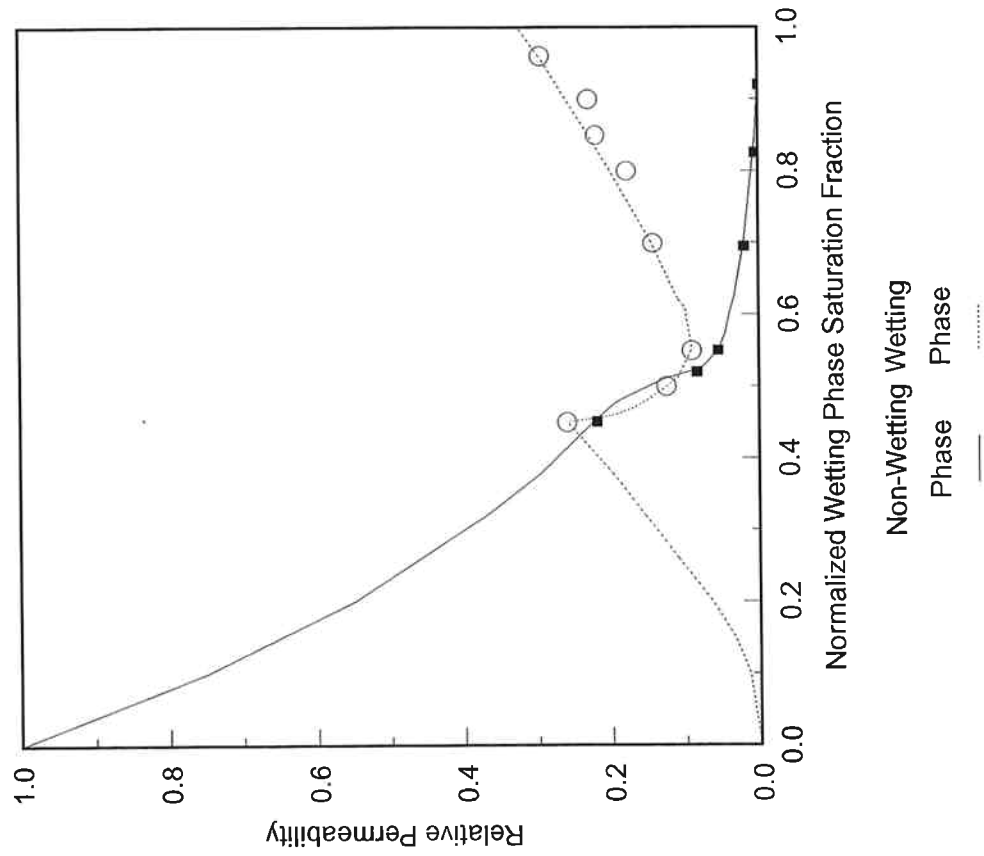


FIGURE 4
COMPARISON OF VARIOUS RELATIVE PERMEABILITY
CURVE CONFIGURATIONS USING EXPONENTIAL
FUNCTION FORMS

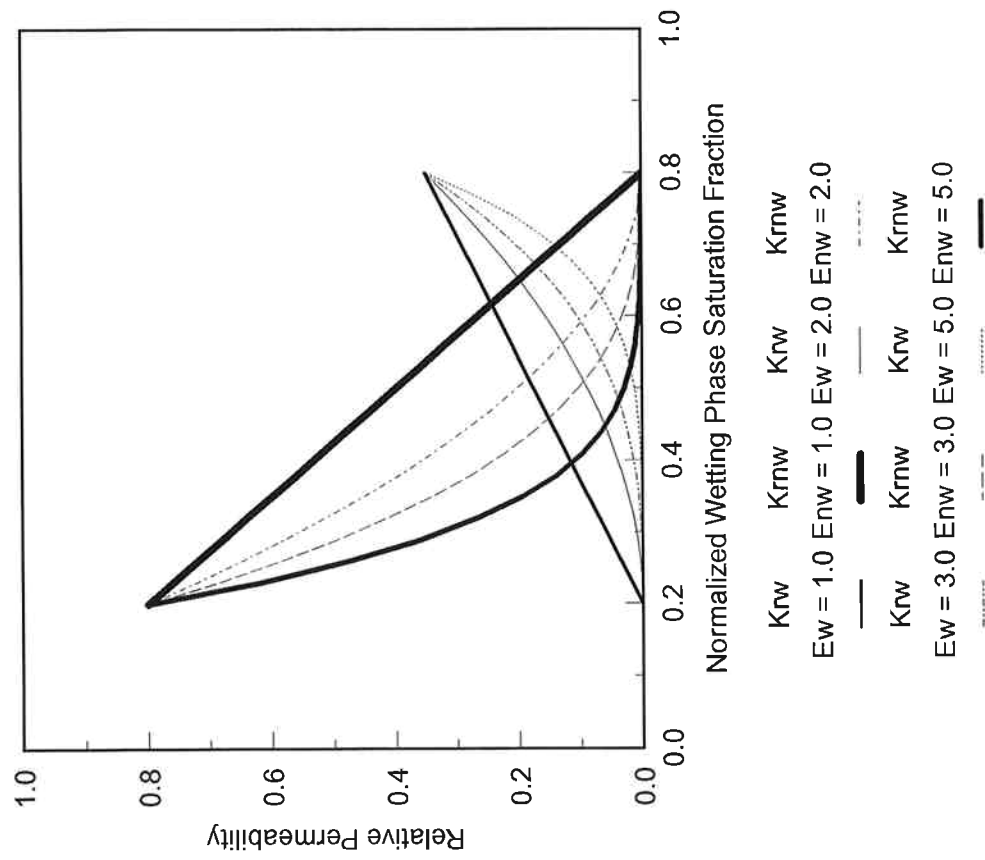


FIGURE 5

EXAMPLES OF RELATIVE PERMEABILITY CURVE CONFIGURATIONS GENERATED USING CUBIC SPLINE FUNCTIONAL FORMS

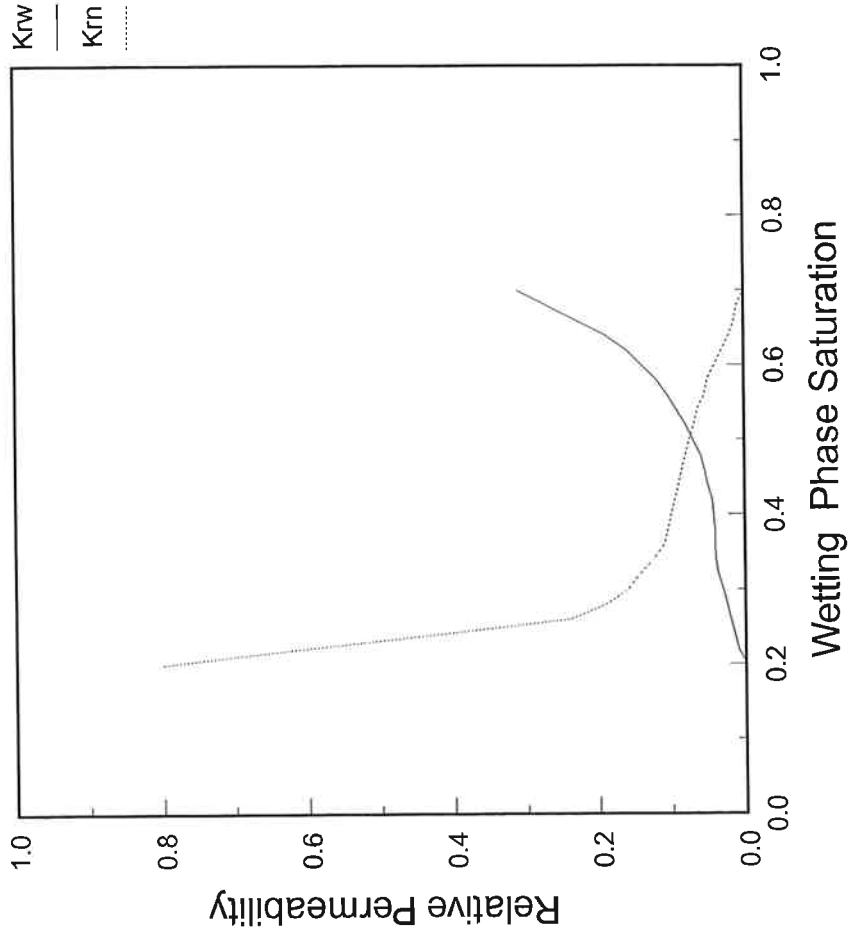
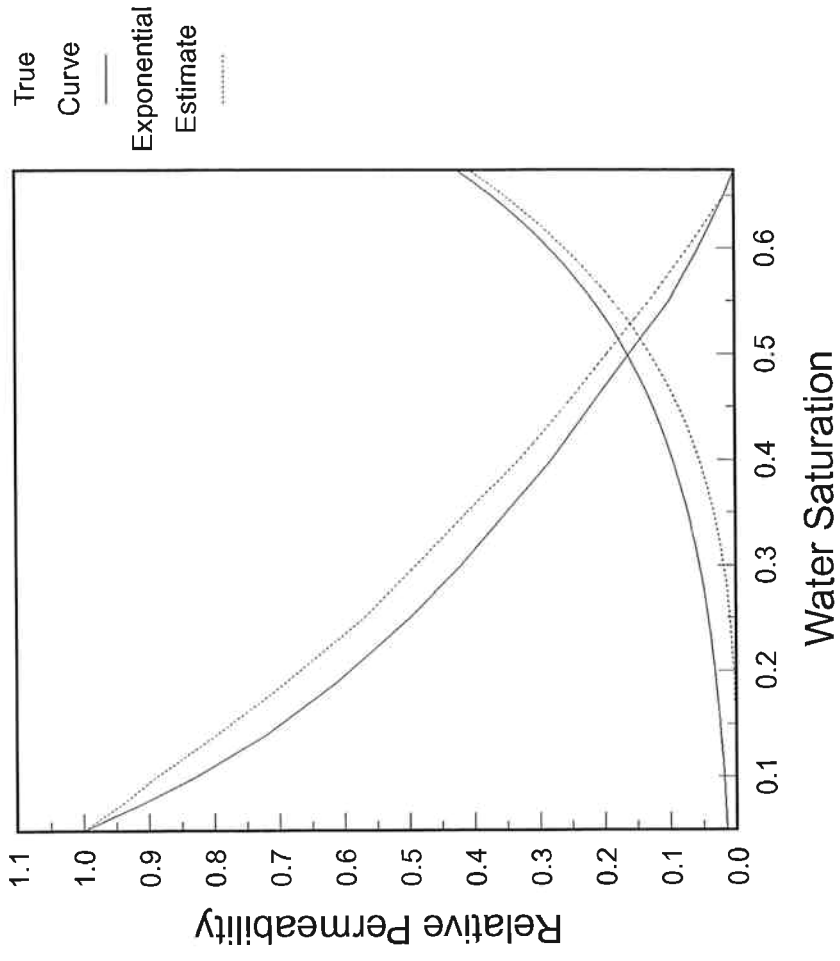


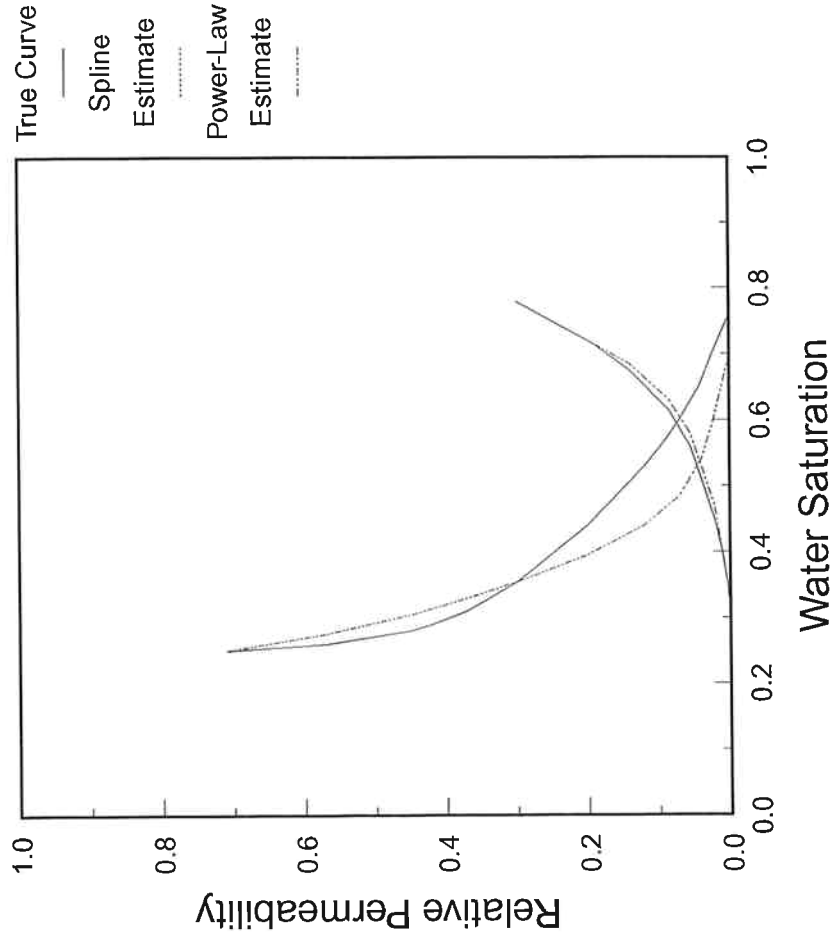
FIGURE 6

ILLUSTRATION OF BIAS ERROR ASSOCIATED WITH THE USE OF EXPONENTIAL FUNCTIONAL FORMS FOR RELATIVE PERMEABILITIES IN AUTOMATIC HISTORY MATCHING



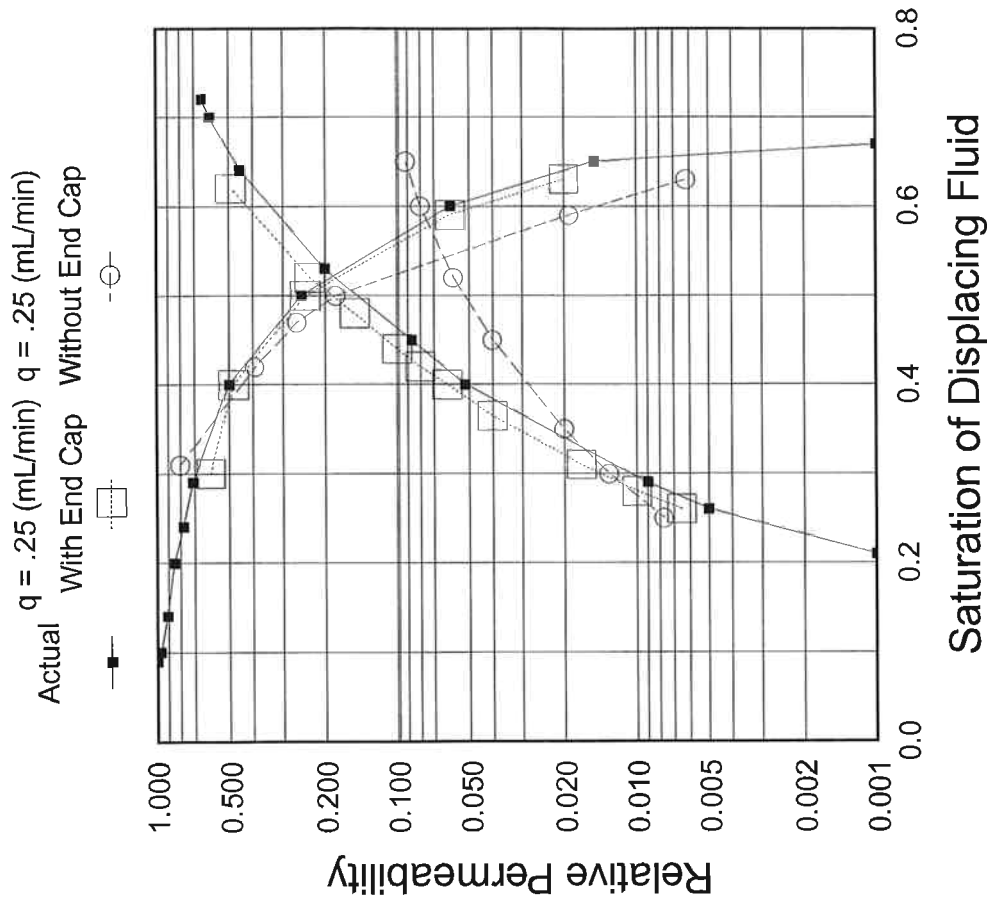
From Kerig et al (Ref 37)

FIGURE 7
COMPARISON OF EXPONENTIAL AND SPLINE
FUNCTIONAL FORMS FOR GENERATING RELATIVE
PERMEABILITY CURVES BY THE AUTOMATIC
HISTORY MATCHING METHOD



From Watson et al (Ref 42)

FIGURE 8
EFFECT OF AN OUTLET SECTION IN NEGATING
CAPILLARY END EFFECT



From Fassihi (Ref 44)

FIGURE 9
EFFECT OF RATE IN NEGATING CAPILLARY END
EFFECTS

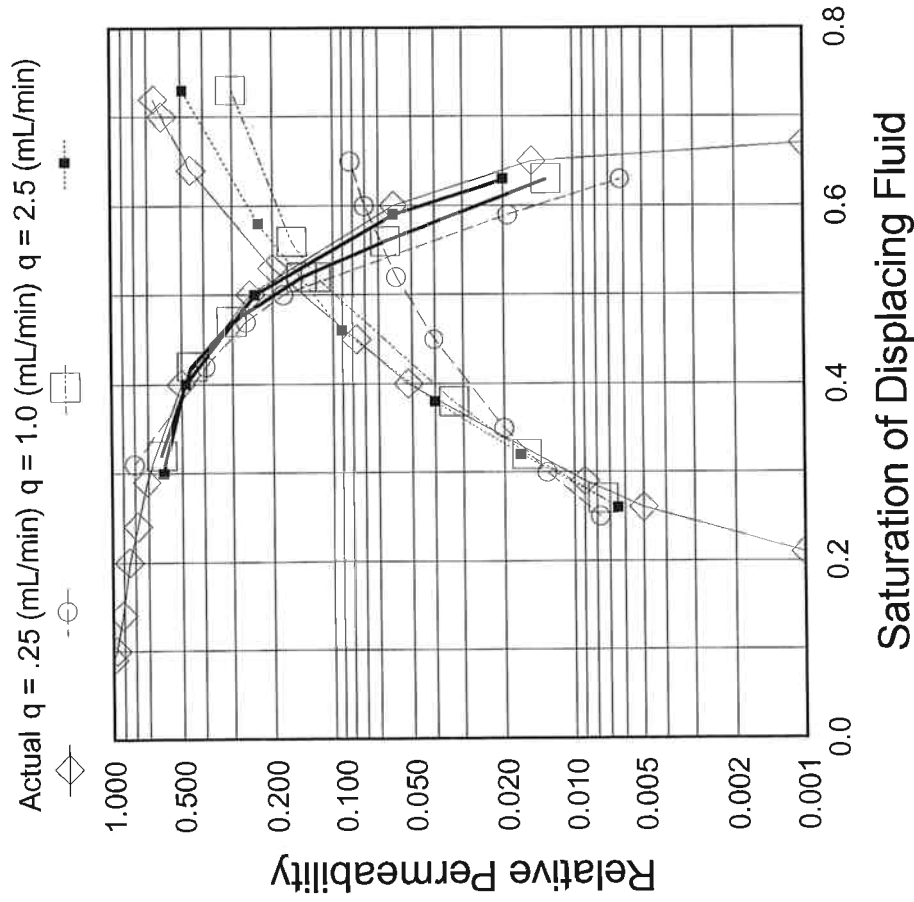


FIGURE 10
ILLUSTRATION OF POTENTIAL CONFIGURATIONS
OF PERMEABILITY PROFILES FROM ELEVATED
RATE DISPLACEMENT TESTS FOR ENDPOINT
CORRECTION

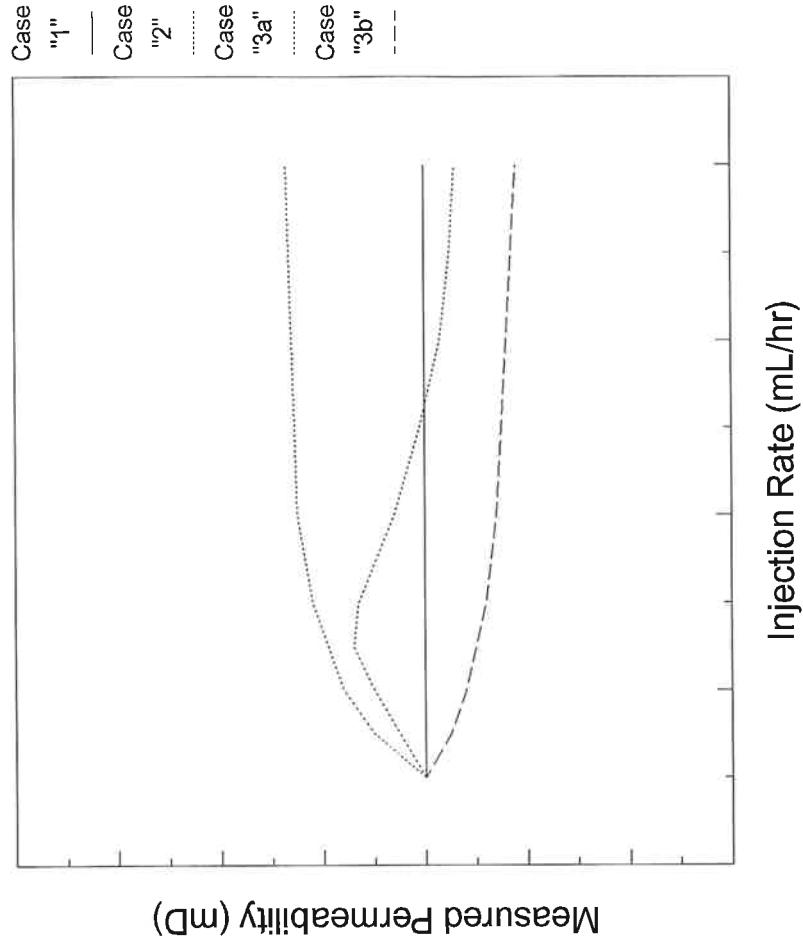


FIGURE 11
ENDPOINT CORRECTION TEST DATA
WATER-OIL TESTS

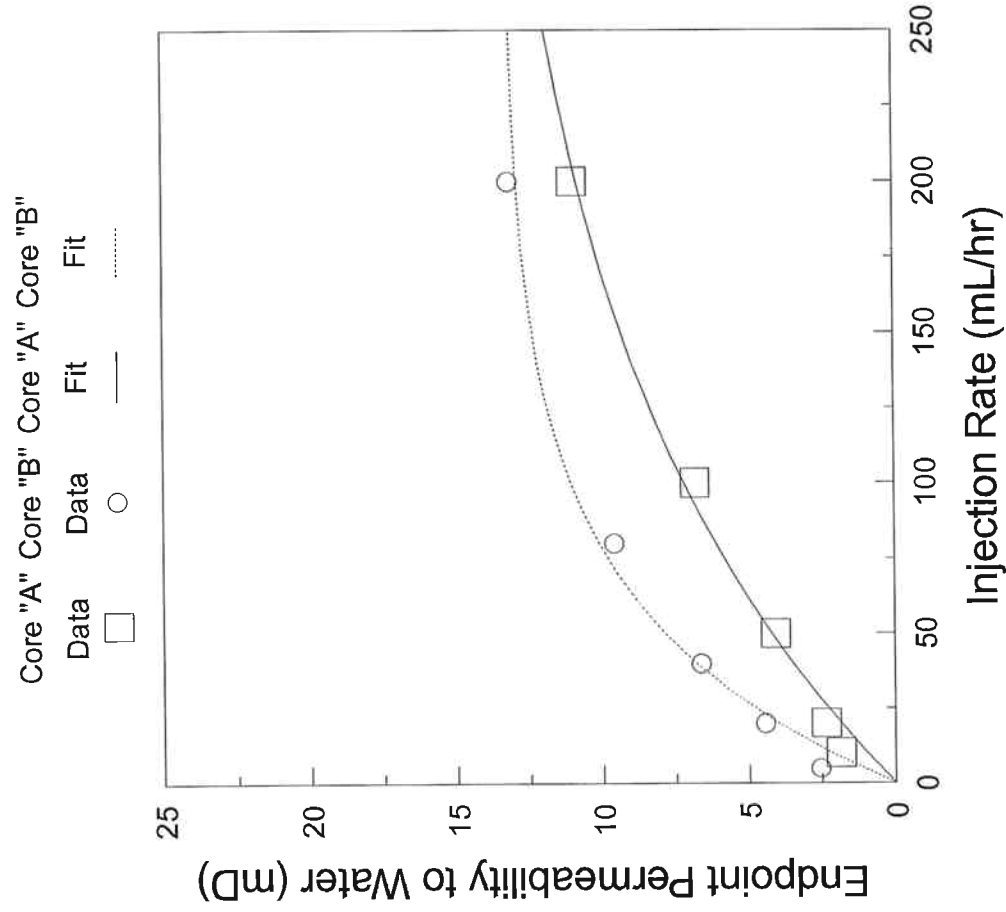


FIGURE 12
ENDPOINT CORRECTION TEST DATA
GAS-OIL TESTS

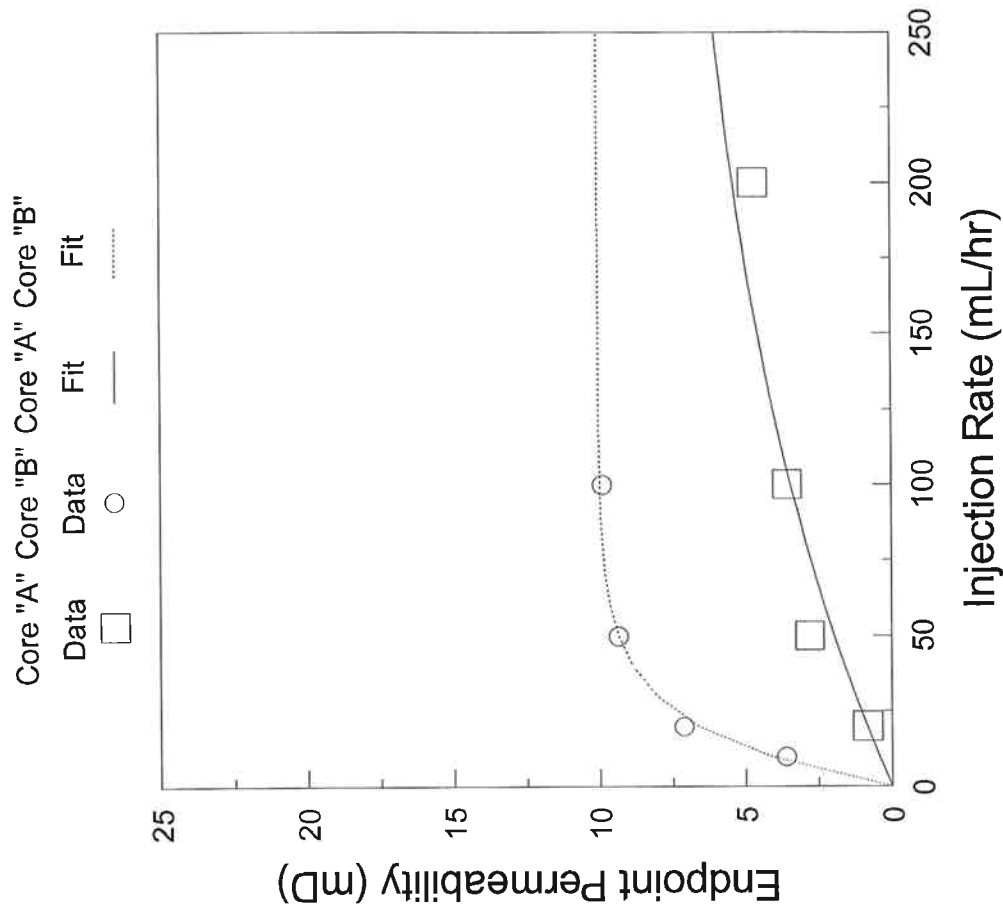


FIGURE 13
EXAMPLE OF APPLICATION OF ENDPOINT CORRECTION
METHOD FOR THE CASE OF A CHANGE IN ENDPOINT
RESIDUAL SATURATION

